Applied Physics Letters

RESEARCH ARTICLE | FEBRUARY 06 2023

Probing itinerant carrier dynamics at the diamond surface using single nitrogen vacancy centers

Marjana Mahdia ; James Allred; Zhiyang Yuan ; Jared Rovny ; Nathalie P. de Leon

Appl. Phys. Lett. 122, 064002 (2023)
https://doi.org/10.1063/5.0130761

AIP Publishing

Applied Physics Letters ARTICLE scitation.org/journal/apl

Probing itinerant carrier dynamics at the diamond surface using single nitrogen vacancy centers

Cite as: Appl. Phys. Lett. **122**, 064002 (2023); doi: 10.1063/5.0130761
Submitted: 14 October 2022 · Accepted: 22 December 2022 ·
Published Online: 6 February 2023

Marjana Mahdia, James Allred, Zhiyang Yuan, Jared Rovny, and Nathalie P. de Leon[a)]

AFFILIATIONS

Department of Electrical and Computer Engineering, Princeton University, Princeton, New Jersey 08544, USA

[a)]Author to whom correspondence should be addressed: npdeleon@princeton.edu

ABSTRACT

Color centers in diamond are widely explored for applications in quantum sensing, computing, and networking. Their optical, spin, and charge properties have extensively been studied, while their interactions with itinerant carriers are relatively unexplored. Here, we show that NV centers situated 10 ± 5 nm of the diamond surface can be converted to the neutral charge state via hole capture. By measuring the hole capture rate, we extract the capture cross section, which is suppressed by proximity to the diamond surface. The distance dependence is consistent with a carrier diffusion model, indicating that the itinerant carrier lifetime can be long, even at the diamond surface. Measuring dynamics of near-surface NV centers offers a tool for characterizing the diamond surface and investigating charge transport in diamond devices.

Color centers have widely been studied for their applications in quantum sensing, quantum networks, and quantum information processing.[1–3] Nitrogen vacancy (NV) centers in diamond, in particular, are an attractive platform because they exhibit long spin coherence times at room temperature and they allow for off-resonant optical detection and initialization of spin states.[1,4] Charge state stability and control of NV centers are of particular interest for applications in nanoscale sensing,[5,6] superresolution microscopy,[7] and long-term data storage.[8] Recent experiments have focused on selectively preparing[9–12] and reading out[13–15] particular charge states as well as studying the impact of charge dynamics on optically detected magnetic resonance.[16,17] However, the interactions between itinerant carriers and color centers are less well explored and can strongly impact the color center charge state, ionization dynamics, and spin readout. Such interactions could also be harnessed for recently developed functionality, such as electrically detected magnetic resonance,[18,19] and stabilizing non-equilibrium charge distributions.[20,21]

Recent work has focused on using itinerant carriers to manipulate color centers in the diamond bulk. For example, it was shown that the optically dark state of a silicon vacancy (SiV) center is SiV^{2-} through charge state readout of NV centers and SiV centers combined with remote optical pumping.[22] In another example, holes generated by one NV center were captured by another NV center, converting the latter NV center to the neutral charge state.[23] Both studies examined NV centers far ($>10\,\mu$m) from the surface, at which distances surface effects are negligible.

Here, we study charge dynamics of shallow NV centers (10 ± 5 nm from the surface) and their interaction with itinerant carriers. Shallow defects are essential for high sensitivity quantum sensing, and understanding the NV charge state and itinerant carrier dynamics near the surface is critical for developing shallow NV centers as a quantum platform. We demonstrate that the charge state of a shallow probe NV center (NV_P) can be controlled by free carriers generated by excitation of another remote shallow source NV center (NV_S) up to $\sim 7\,\mu$m away [Figs. 1(a) and 1(b)]. Specifically, the charge state of NV_P converts from negative to neutral as a second 532 nm excitation laser is scanned over NV_S [Fig. 1(c)]. Continuous optical ionization and recombination of NV_S generate a constant flow of holes and electrons in the valence and conduction bands, respectively. These itinerant carriers can diffuse and subsequently be captured by NV_P. The net conversion to the neutral charge state implies that hole capture is much more efficient than electron capture, leading to a net change in the steady-state charge. This phenomenon has been observed in some previous works.[22,23]

NV centers are individually interrogated using a dual channel, multicolor confocal microscope (see the supplementary material for details). In the experiment, two optically resolvable NV centers are chosen within the scanning field of view, NV_P and NV_S. One optical channel monitors the charge state of NV_P after initialization into NV^- with roughly 70% probability using a high power green pulse (94 μW, 5 ms), followed by charge state readout with a low power orange pulse

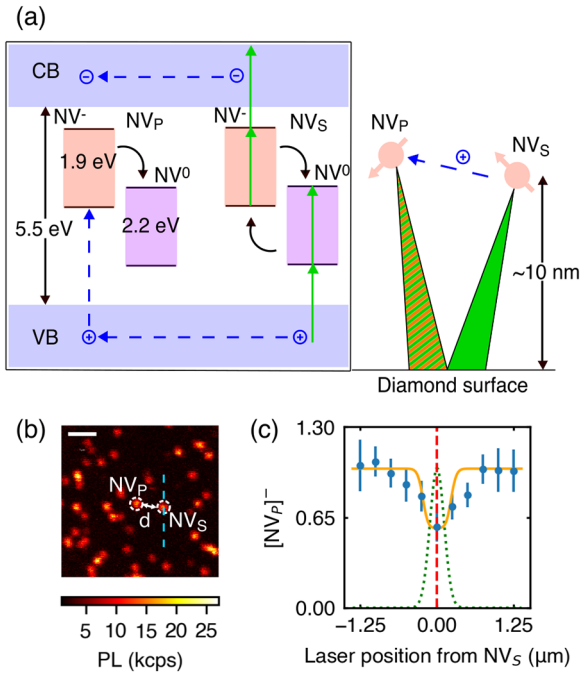

FIG. 1. (a) Energy level diagram showing charge state conversion processes between NV_S and NV_P. The solid vertical arrows indicate photoionization processes, the dashed arrows indicate itinerant carrier transport and capture, and the curved arrows indicate charge state conversion. (b) Scanning confocal microscope image of two NV centers. The scale bar is 1 μm. (c) The NV^- charge state population of NV_P as a second laser is scanned along the line cut shown in (b) with the NV_S position indicated with the red dashed line. The orange solid line is a fit considering the dependence of $[NV_P]^-$ on the NV_S excitation laser power. The laser spot size is indicated for reference (green dotted line).

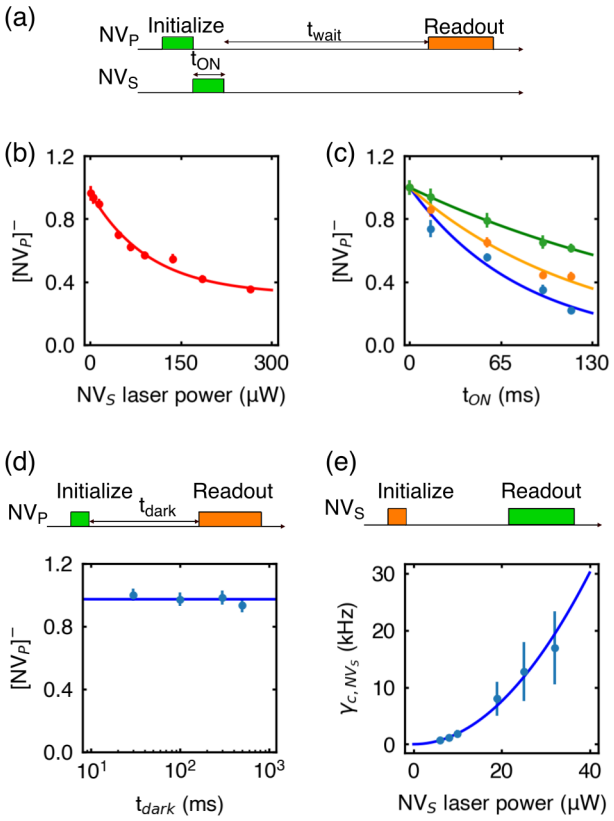

FIG. 2. (a) Pulse sequence used to detect the change in the NV_P charge state due to optical excitation of NV_S. A 532 nm laser pulse (94 μW, 5 ms) initializes NV_P. Another 532 nm pulse (variable power) continuously drives ionization and recombination processes of NV_S for t_{ON}. A 591 nm laser pulse (2 μW, 150 ms) is used to readout the charge state of NV_P. A wait time, $t_{wait} = 15$ ms is introduced to avoid background phosphorescence from optical components. (b) Dependence of $[NV_P]^-$ on NV_S excitation laser power ($t_{ON} = 15$ ms). The solid line indicates an exponential fit. (c) $[NV_P]^-$ as a function of t_{ON} for different NV_S excitation laser powers (green: 138 μW, orange: 168 μW, and blue: 216 μW), $d = 2.6$ μm. Solid lines indicate exponential fits, where the NV_P hole capture probability approaches unity as t_{ON} reaches ∞. (d) The stability of the $[NV_P]^-$ in the dark. No change is detected out to 500 ms. (e) Hole generation rate (γ_c) vs green (readout) laser power for NV_S. The fit curve is quadratic, indicating a two photon process.

(2 μW, 150 ms). In between these pulses, the second optical channel is used to pump NV_S for a time t_{ON} with a green laser pulse of variable power, cycling its charge state between NV^- and NV^0 [Fig. 2(a)]. This cycling generates free carriers that diffuse away and can be subsequently captured by nearby NV centers. The charge state population is measured by obtaining fluorescence with orange excitation since 591 nm is situated in between the zero phonon lines (ZPL) of NV^- (637 nm) and NV^0 (575 nm). A time window shorter than the decay time obtained from the fluorescence trace is defined, over which a histogram of photon counts is drawn. The area under the double Poisson shaped histogram is used to determine the charge state population of NV_P (see the supplementary material for details).

We interrogate the charge capture kinetics by measuring the charge state of NV_P while varying the excitation power at NV_S. As the excitation power increases, the negative charge state population ($[NV_P]^-$) (normalized with respect to the NV^- population just after initialization with the green laser) decreases [Fig. 2(b)]. Moreover, $[NV_P]^-$ decays exponentially with the duration of the NV_S excitation pulse, and the decay time constant decreases with increasing excitation power [Fig. 2(c)]. Without any excitation at NV_S, there is no change in $[NV_P]^-$ over time [Fig. 2(d)]. The net decay of $[NV_P]^-$ during NV_S illumination indicates that hole capture in the negative charge state dominates over electron capture in both the negative and neutral charge states.

We model the hole capture rate, γ_h as

$$\begin{aligned}\gamma_h &= \rho_h c_h + \gamma_d, \\ &= \frac{2\gamma_c e^{-d/L_h}}{4\pi d^2 \nu_h}\sigma_h \nu_h + \gamma_d, \\ &= \frac{\sigma_h}{2\pi d^2}\gamma_c e^{-d/L_h} + \gamma_d,\end{aligned} \tag{1}$$

where ρ_h is the hole density, c_h is the capture coefficient, γ_c is the hole generation rate at NV_S, L_h is an effective hole diffusion length that arises from the free carrier lifetime, d is the distance between NV_S and NV_P, σ_h is the hole capture cross section at NV_P, ν_h is the hole velocity, and γ_d is the dark ionization rate, which is constant. The factor of two in the numerator of Eq. (1) arises from a geometrical factor—we assume that carriers can reflect from the surface, and the NV centers

are much closer to the surface than they are to each other. To calculate γ_c [Fig. 2(e)], we first fit the fluorescence of NV_S under 532 nm illumination (after initialization with 591 nm laser) to an exponential fit to extract the total charge conversion rate, $\gamma_{total} = \gamma_i + \gamma_r$ of NV_S, where γ_i and γ_r are ionization and recombination rates, respectively[16] (see the supplementary material for details). We measure the NV^- population of several NV centers in our sample at the steady state for several powers of 532 nm initialization. All of the measured NV centers show NV^- population in the range of [55%, 70%], which along with γ_{total} is used to calculate γ_r and subsequently γ_i. In the steady state, since the time between subsequent holes is the total time it takes for a hole and an electron to be generated, we have $\gamma_c = (1/\gamma_i + 1/\gamma_r)^{-1}$.

We measured 17 pairs of NV centers in total and observed hole capture in 14 of the pairs [Fig. 3(a)]. For the three pairs of NV centers in which we did not observe hole capture, we were unable to determine any particular characteristics that account for their behavior. More detailed characterization of the variation in microscopic local environment could reveal other confounding factors, such as the presence of other carrier traps. For the remaining 14 pairs, the hole capture rate varies among pairs of NV centers and is generally slower for NV pairs with larger spacing d [Fig. 3(b)]. This distance dependence could arise from the area scaling of carrier diffusion or from a finite carrier lifetime. By rearranging Eq. (1), we can define a parameter α to investigate if the hole carrier lifetime is an important factor where

$$\alpha = \frac{\gamma_h - \gamma_d}{\gamma_c} = \frac{\sigma_h e^{-d/L_h}}{2\pi d^2}. \quad (2)$$

We assume $\gamma_d = 0$ because the run time of the experiment (<600 ms) is shorter than the dark lifetime of NV_P [Fig. 2(c), see the supplementary material for details]. The calculated α for each NV pair is plotted vs inter-NV distance in Fig. 3(c). The distance dependence is consistent with a $1/d^2$ scaling (see the supplementary material for details). We, therefore, conclude that the effective ionization of NV_P due to NV_S is not limited by the diffusion length of holes.

From the fit in Fig. 3(c), we extract the capture cross section, $\sigma_h = 2.89 \times 10^{-4} \pm 0.54 \times 10^{-4}$ μm^2. The large value of σ_h likely arises from the Coulomb attraction between the negatively charged NV center and the hole, resulting in Rydberg-like states.[24] We note that although the cross section is large, this value is an order of magnitude smaller than previously reported for deep NV centers.[23] The surface-related suppression of hole capture could arise from finite hole lifetime due to surface traps or reduction in the effective cross section because of geometric overlap with the surface. We rule out the former reason based on the distance dependence shown in Fig. 3(c). We note that while our model accounts for the overall distance trend in the data, there remains substantial scatter within the dataset that could arise from differences in the microscopic environment of each NV center. An interesting area of future research would be to perform detailed spectroscopy to uncover the sources of this variation.

In summary, we have demonstrated generation and capture of free carriers between two shallow NV centers that are <10 μm apart from one another. We have shown that the hole capture cross section is smaller than prior measurements of bulk NV centers but that the observed carrier capture rate is not limited by the carrier lifetime. The hole diffusion length and hole capture cross section can be utilized as sensitive probes of charge transport in diamond devices. The technique demonstrated here can be easily extended to stabilize particular charge states of defects through photo-doping with distant donors, rather than bulk doping, as we have recently demonstrated for SiV^0 centers.[21] A natural next step would be to deploy photodoping to stabilize new color centers, such as GeV^0, SnV^0, and PbV^0.

See the supplementary material for details about methods, determination of NV^- population, calculation of carrier generation rate, measurement of dark ionization rate, verification of long diffusion length, and hole capture rates for concerned NV centers.

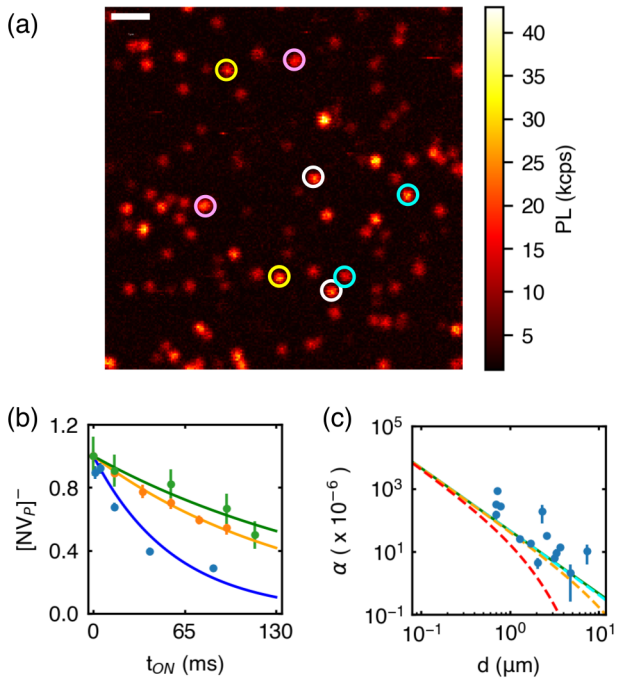

FIG. 3. (a) Confocal scan showing a subset of the NV pairs investigated for calculating σ_h and L_h. Pairs are indicated by different colors. The scale bar is 1 μm. (b) Time-dependent decay of $[NV_P]^-$ varies with d (green: 1.71 μm, orange: 1.29 μm, and blue: 0.70 μm). NV_S is excited with a 90 μW 532 nm laser. Solid lines indicate exponential fits, whereas t_{ON} reaches ∞, the probability of hole capture approaches unity. (c) The ratio of the hole capture rate to the hole generation rate, α, for the 14 different NV pairs under study. The distance dependence is consistent with a diffusion model with an infinite diffusion length (green solid line). For comparison, three dashed lines with finite L_h (cyan: 100 μm, orange: 10 μm, and red: 1 μm) are also included.

The authors would like to thank Carlos Meriles and Artur Lozovoi for helpful discussions. This work was primarily supported by the U.S. Department of Energy, Office of Science, Office of Basic Energy Sciences, under Award No. DE-SC0018978. The diamond surface preparation was supported by the NSF under the CAREER program (Grant No. DMR1752047). J.A. acknowledges the NSF Graduate Research Fellowship Program for support. J.R. acknowledges the Princeton Quantum Initiative Postdoctoral Fellowship for support.

AUTHOR DECLARATIONS

Conflict of Interest

The authors have no conflicts to disclose.

Author Contributions

Marjana Mahdia: Conceptualization (equal); Data curation (equal); Formal analysis (equal); Investigation (equal); Software (equal); Visualization (equal); Writing – original draft (equal); Writing – review & editing (equal). **James Allred:** Conceptualization (equal); Data curation (equal); Formal analysis (equal); Investigation (equal); Methodology (equal); Visualization (equal); Writing – original draft (equal); Writing – review & editing (equal). **Zhiyang Yuan:** Data curation (equal); Formal analysis (supporting); Investigation (supporting); Software (supporting); Validation (equal); Writing – original draft (supporting); Writing – review & editing (supporting). **Jared Rovny:** Conceptualization (supporting); Data curation (equal); Formal analysis (equal); Supervision (supporting); Validation (equal); Writing – original draft (supporting); Writing – review & editing (equal). **Nathalie de Leon:** Conceptualization (equal); Data curation (equal); Formal analysis (equal); Funding acquisition (equal); Investigation (equal); Methodology (equal); Project administration (equal); Resources (equal); Supervision (equal); Validation (equal); Writing – original draft (equal); Writing – review & editing (equal).

DATA AVAILABILITY

The data that support the findings of this study are available from the corresponding author upon reasonable request.

REFERENCES

[1]L. Childress and R. Hanson, MRS Bull. **38**, 134 (2013).
[2]S. Hong, M. S. Grinolds, L. M. Pham, D. Le Sage, L. Luan, R. L. Walsworth, and A. Yacoby, MRS Bull. **38**, 155 (2013).
[3]R. Schirhagl, K. Chang, M. Loretz, and C. L. Degen, Annu. Rev. Phys. Chem. **65**, 83 (2014).
[4]N. Bar-Gill, L. M. Pham, A. Jarmola, D. Budker, and R. L. Walsworth, Nat. Commun. **4**(1), 1743 (2013).
[5]T. Staudacher, F. Shi, S. Pezzagna, J. Meijer, J. Du, C. A. Meriles, F. Reinhard, and J. Wrachtrup, Science **339**, 561 (2013).
[6]H. Mamin, M. Kim, M. Sherwood, C. Rettner, K. Ohno, D. Awschalom, and D. Rugar, Science **339**, 557 (2013).
[7]X. Chen, C. Zou, Z. Gong, C. Dong, G. Guo, and F. Sun, Light: Sci. Appl. **4**, e230 (2015).
[8]S. Dhomkar, J. Henshaw, H. Jayakumar, and C. A. Meriles, Sci. Adv. **2**, e1600911 (2016).
[9]C. Kurtsiefer, S. Mayer, P. Zarda, and H. Weinfurter, Phys. Rev. Lett. **85**, 290 (2000).
[10]L. Rondin, G. Dantelle, A. Slablab, F. Grosshans, F. Treussart, P. Bergonzo, S. Perruchas, T. Gacoin, M. Chaigneau, H.-C. Chang *et al.*, Phys. Rev. B **82**, 115449 (2010).
[11]S. Cui and E. L. Hu, Appl. Phys. Lett. **103**, 051603 (2013).
[12]C. Schreyvogel, V. Polyakov, R. Wunderlich, J. Meijer, and C. Nebel, Sci. Rep. **5**, 12160 (2015).
[13]P. Neumann, J. Beck, M. Steiner, F. Rempp, H. Fedder, P. R. Hemmer, J. Wrachtrup, and F. Jelezko, Science **329**, 542 (2010).
[14]L. Robledo, L. Childress, H. Bernien, B. Hensen, P. F. Alkemade, and R. Hanson, Nature **477**, 574 (2011).
[15]B. J. Shields, Q. P. Unterreithmeier, N. P. de Leon, H. Park, and M. D. Lukin, Phys. Rev. Lett. **114**, 136402 (2015).
[16]Z. Yuan, M. Fitzpatrick, L. V. Rodgers, S. Sangtawesin, S. Srinivasan, and N. P. de Leon, Phys. Rev. Res. **2**, 033263 (2020).
[17]D. Bluvstein, Z. Zhang, and A. C. B. Jayich, Phys. Rev. Lett. **122**, 076101 (2019).
[18]F. M. Hrubesch, G. Braunbeck, M. Stutzmann, F. Reinhard, and M. S. Brandt, Phys. Rev. Lett. **118**, 037601 (2017).
[19]P. Siyushev, M. Nesladek, E. Bourgeois, M. Gulka, J. Hruby, T. Yamamoto, M. Trupke, T. Teraji, J. Isoya, and F. Jelezko, Science **363**, 728 (2019).
[20]S. Dhomkar, P. R. Zangara, J. Henshaw, and C. A. Meriles, Phys. Rev. Lett. **120**, 117401 (2018).
[21]Z.-H. Zhang, A. M. Edmonds, N. Palmer, M. L. Markham, and N. P. de Leon, arXiv:2209.08710 (2022).
[22]A. Gardill, I. Kemeny, M. C. Cambria, Y. Li, H. T. Dinani, A. Norambuena, J. R. Maze, V. Lordi, and S. Kolkowitz, Nano Lett. **21**, 6960 (2021).
[23]A. Lozovoi, H. Jayakumar, D. Daw, G. Vizkelethy, E. Bielejec, M. W. Doherty, J. Flick, and C. A. Meriles, Nat. Electron. **4**, 717 (2021).
[24]Z.-H. Zhang, P. Stevenson, G. Thiering, B. C. Rose, D. Huang, A. M. Edmonds, M. L. Markham, S. A. Lyon, A. Gali, and N. P. De Leon, Phys. Rev. Lett. **125**, 237402 (2020).